AIP | Applied Physics Letters

Spectral tunability of realistic plasmonic nanoantennas

Alejandro Portela, Takaaki Yano, Christian Santschi, Hiroaki Matsui, Tomohiro Hayashi, Masahiko Hara, Olivier J. F. Martin, and Hitoshi Tabata

Citation: Applied Physics Letters **105**, 091105 (2014); doi: 10.1063/1.4894633
View online: http://dx.doi.org/10.1063/1.4894633
View Table of Contents: http://scitation.aip.org/content/aip/journal/apl/105/9?ver=pdfcov
Published by the AIP Publishing

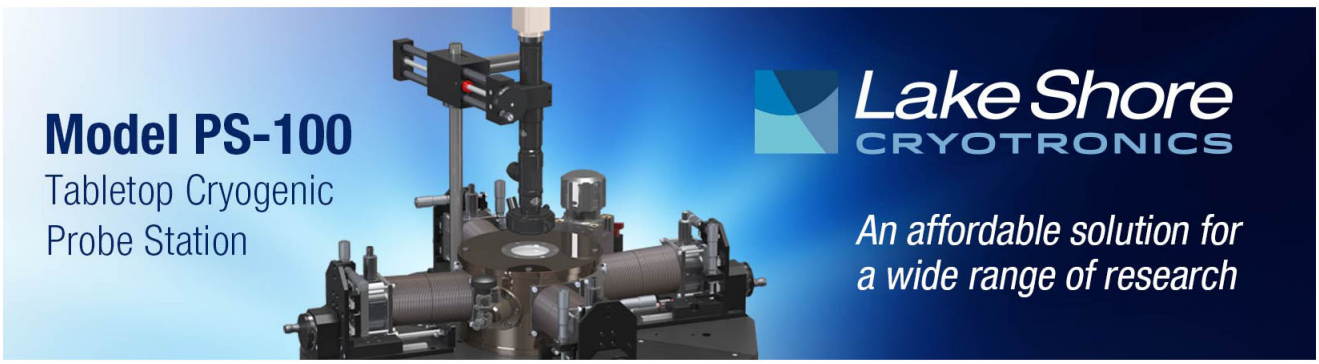

Spectral tunability of realistic plasmonic nanoantennas

Alejandro Portela,[1] Takaaki Yano,[2] Christian Santschi,[3] Hiroaki Matsui,[1] Tomohiro Hayashi,[2] Masahiko Hara,[2] Olivier J. F. Martin,[3] and Hitoshi Tabata[1,a)]
[1]*Department of Bioengineering, School of Engineering, The University of Tokyo, Bunkyo-ku, Tokyo 113-8656, Japan*
[2]*Department of Electronic Chemistry, Tokyo Institute of Technology, Midori-ku, Yokohama, Kanagawa 226-8502, Japan*
[3]*Nanophotonics and Metrology Laboratory, Swiss Federal Institute of Technology Lausanne, Lausanne CH-1015, Switzerland*

(Received 17 July 2014; accepted 22 August 2014; published online 3 September 2014)

Single nanoantenna spectroscopy was carried out on realistic dipole nanoantennas with various arm lengths and gap sizes fabricated by electron-beam lithography. A significant difference in resonance wavelength between realistic and ideal nanoantennas was found by comparing their spectral response. Consequently, the spectral tunability (96 nm) of the structures was significantly lower than that of simulated ideal nanoantennas. These observations, attributed to the nanofabrication process, are related to imperfections in the geometry, added metal adhesion layer, and shape modifications, which are analyzed in this work. Our results provide important information for the design of dipole nanoantennas clarifying the role of the structural modifications on the resonance spectra, as supported by calculations. © *2014 AIP Publishing LLC*. [http://dx.doi.org/10.1063/1.4894633]

The optical properties of metallic plasmonic nanoparticles (NPs) have been investigated for their potential applications in the field of biosensing, especially plasmon enhanced spectroscopies.[1–4] The localized plasmon resonance of metallic NPs shows a high tunability by varying the size, shape, material, and dielectric environment of the NPs.[5,6] The close proximity of two or more metallic NPs induces the plasmon coupling between NPs, leading to the formation of new hybrid plasmon modes.[7] Gapped nanostructures, as sketched in the inset of Fig. 1, known as dipole nanoantenna, have shown a strong field enhancement, e.g., by evidence of white light continuum generation[8] and their optical response can be tailored.[9] Dynamic control of the tunability using graphene[10] or approaching a nanocrystal to the gap of the antenna[11] has been shown.

Some studies have evaluated the influence of shape variations of antennas produced using current nanofabrication technologies.[12–14] The optical response of these antennas, referred as *realistic nanoantennas*, is significantly different, since they do not consist of two ideal rectangular nanorods separated by a nanogap. Therefore, a more extensive study of such structures is of strong interest in order to optimize sensitivity, reliability, and estimate the limits of plasmonic biosensors.[15] A recent report demonstrates the role of the realistic geometry in the enhancement of fluorescence and Raman scattering.[16]

Biological studies are increasingly requiring molecular identification to clarify important biological processes. Therefore, the optical response of a plasmonic system embedded in a water-based environment is of particular interest. Surface Enhanced Raman Spectroscopy (SERS) represents a powerful tool to observe molecular vibrations, which requires precise control of the plasmon resonance of the antennas to obtain optimum field enhancements.[15]

In this paper, we present a systematic study of optical response of nanofabricated nanogap antennas placed on glass substrate and water environment. Their geometrical parameters, the comparison of the optical responses—specifically the actual tunability properties—are discussed by comparing experimental and theoretical approaches.

Figure 1(a) shows a series of 3D simulations using a Green's tensor method as described elsewhere[9] for ideal nanoantennas using experimental dielectric constants.[17] The antennas arm lengths are varied from 40 to 110 nm, with gap sizes of 20, 30, and 40 nm, respectively. The width and thickness of the antennas were kept constant at 40 nm for a reliable fabrication.[15] The underlying glass substrate is described with dielectric index of $n_s = 1.5$ and the water with assumed index of $n_{env} = 1.33$.

The antennas are illuminated from below under an incident angle of $\theta = 70°$ with a light beam linearly polarized light along the main axis of the antenna. A triangular mesh of 2 nm was used for determining the intensity enhancement and the antenna's spectral response. The electric field normalized with respect to the incident illumination intensity I_0 is calculated at the center of the feed-gap where the intensity is maximum, as indicated by a black mark in the inset of Fig. 1(a). The calculated optical response of such nanoantennas shows a strong dependency on structural dimensions. Particularly, a decrease of the gap size results in a high intensity enhancement, Fig. 1(b). The resonant peak position quasi-linearly increases with an increase of the length of the nanoantenna, Fig. 1(c).

Nanoantennas were fabricated by electron-beam (EB) lithography using lift-off process on glass substrate, as shown in Fig. 2. A double layer of photoresists with different thickness is spin-coated (methylmethacrylate 120 nm and polymethylmethacrylate 60 nm) in order to form a cavity with a small undercut after exposition to a 100 keV EB (Vistec, EBPG5000). This is followed by the developing of the resists

a)Author to whom correspondence should be addressed. Electronic mail: tabata@bioeng.t.u-tokyo.ac.jp.

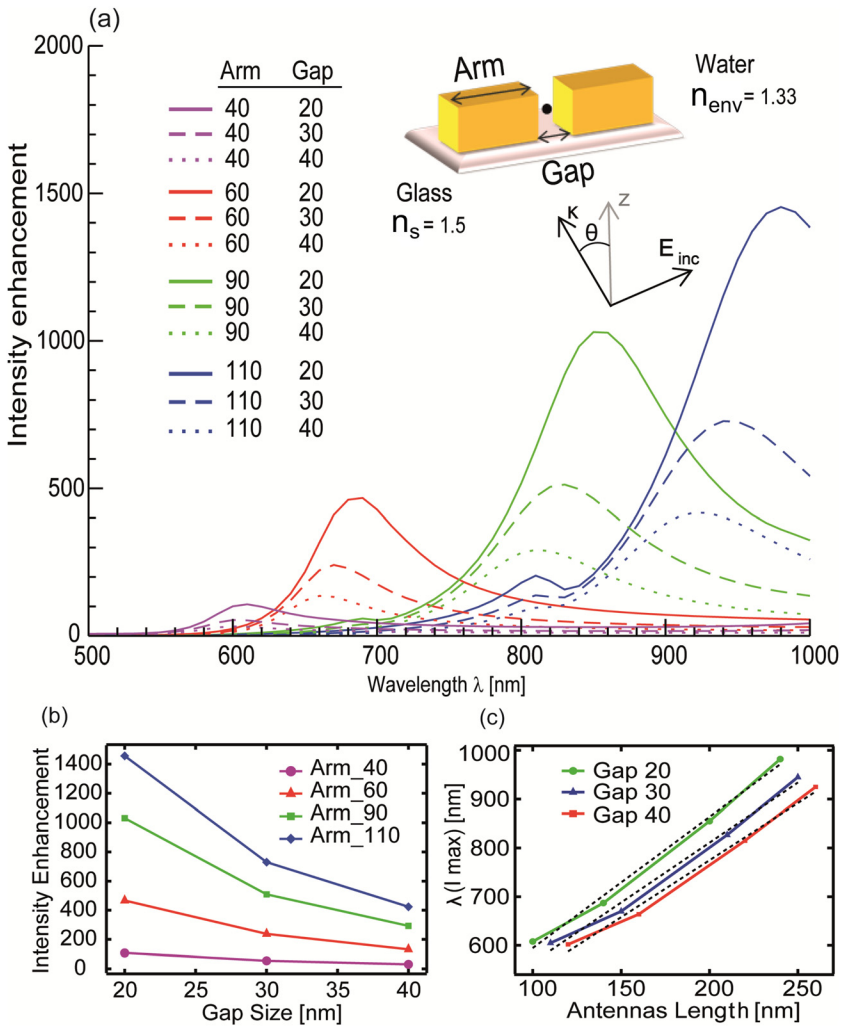

FIG. 1. Ideal plasmonic dipole nanoantennas. (a) Spectral response with different gap sizes and lengths. (b) Intensity enhancement with respect to the incident light, as a function of the gap size for different arm lengths. (c) Resonance peak position as a function of the antenna length. The dashed lines represent the quasi-linear relation between the resonance peak position (λ (Imax) [nm]) and the antenna length.

and the evaporation of a 2 nm Cr adhesion layer and a 40 nm Au layer.

Arrays of antennas are fabricated with 1 μm separation along the vertical and horizontal directions, which is large enough to prevent near-field coupling phenomena. Ten antennas of each pattern (one given arm length and gap size) are measured, resulting in a total of 120 samples. The SEM images of this set were analyzed, obtaining geometrical parameters for comparison with the corresponding design patterns. Table I shows the average measured length for each arm, left "ArmL," right "ArmR," and the actual size gap for intended gap design.

The average arm lengths are sensibly larger than the intended values; however, they show a good repeatability with a standard deviation of 1.7–5.6 nm. The enlargement of the arms produced a shrinking of the gap size in all the patterns, with averages of 16.1 and 36.0 nm for the intended gap sizes of 20 and 40 nm, respectively. These effects are possibly related with the surface diffusion of the Au layer, which

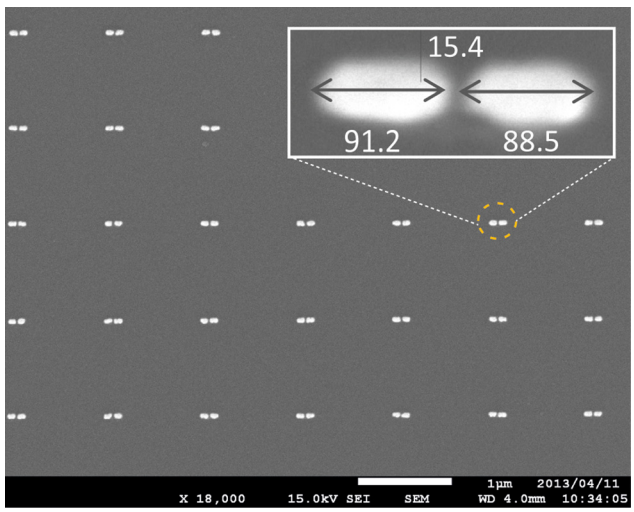

FIG. 2. SEM image of a set of fabricated nanoantennas (80 nm arm length and 20 nm gap); scalebar: 1 μm. The inset shows a magnification of a single antenna.

TABLE I. Average values of arm lengths (nm) and gap for nanoantennas with intended design gap of 20 and 40 nm.

Arm design	ArmL gap_20	Gap 20	ArmR gap_20	ArmL gap_40	Gap 40	ArmR gap_40
40	49.3	15.5	48.4	46.8	35.9	46.7
45	54.3	14.0	54.0	54.1	34.9	52.3
60	67.9	11.7	69.8	68.2	32.9	67.1
75	85.0	16.5	83.2	81.2	39.3	81.1
80	87.5	19.3	85.4	87.6	35.4	88.4
100	106.9	19.4	105.4	107.3	38.6	108.5

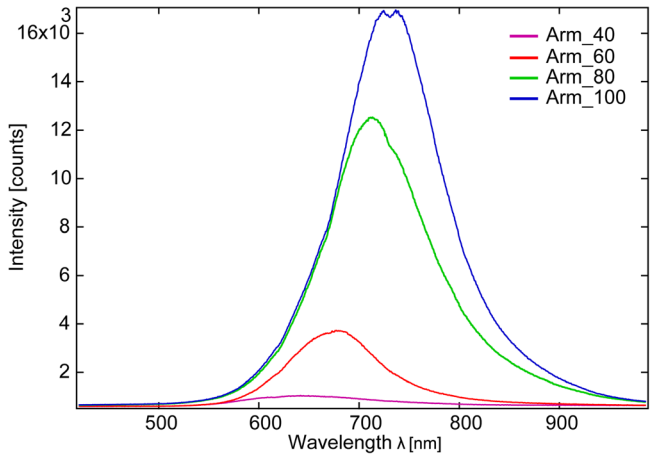

FIG. 3. Optical spectra of the fabricated nanoantennas. The position of the resonance peak is controlled by varying the arm lengths (40, 60, 80, and 100 nm) for a constant gap (20 nm).

is a drawback of the resist cavity undercut that can lead to the lateral diffusion of the deposited metallic layer.

The spectra for variable arm lengths and constant gap size are shown in Fig. 3. The nanoantennas are characterized using a dark-field inverted microscope setup with an oil immersion objective (Plapon 60xO, NA = 1.45 TIRFM, Olympus). The sample was illuminated under total internal reflection using white light and the scattered light was collected using a custom dark-field mirror. This configuration can effectively reduce the background and, hence, achieve an important improvement of the signal to background ratio.

Figure 4 shows the variation of the resonance peak as a function of the total length for two different gap size nanoantennas. First, it confirms a quasi-linear increase of the spectral peak position with the total length of the fabricated nanoantennas. Second, it can be noticed that for the same length, the resonance wavelength is red-shifted for a smaller gap. The shift $\Delta\lambda_g$ remains almost constant over the length range studied in this work and can, therefore, be considered in a first approximation, as independent of the total length of the nanoantenna.

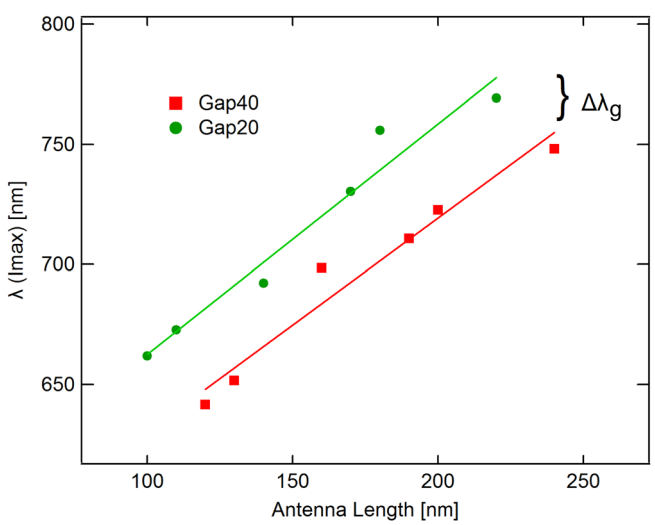

FIG. 4. Tunable response of a set of nanoantennas with gap sizes of 20 and 40 nm and variable length.

However, a significant discrepancy was observed between the response of realistic nanoantennas and the calculations, as illustrated in Fig. 5. The peak position for this gap size nanoantenna can be tuned within a range of 96 nm by changing the total length of the antenna from 110 to 220 nm. This corresponds to a reduction of the tunability of about four times compared to the numerical results for ideal structures. Figure 5 reveals that, with respect to the numerical spectra, antennas having a smaller arm than 60 nm suffer from a red-shift, whereas those with a larger arm undergo a blue-shift.

Antennas with arm length below 60 nm showed a broader spectral line-width, larger dispersion of peak positions, and weaker signal due to the small scattering cross-section resulting in a lower signal to noise ratio. Whereas, for the longer length antennas, the optical response is characterized by a uniform and monotonous decrease of the spectral peak position compared to the simulated ideal structures.

As discussed in Figs. 1(a) and 1(c) and Table I, the observed systematic increase of the arm length and the decrease of gap size should consequently lead to a red-shift of the resonance peak position. Thus, despite the high ability to achieve spectral tailoring modifying these parameters, the effects related to the nanofabrication process can deteriorate the tunability of realistic nanoantennas. Among them, the influence of the adhesion layer deposited before the Au evaporation has been considered and reported to mainly rely on two factors: refractive index and absorption of the material.[18] Siegfried *et al.* recently quantified the effect of adding such interface layer.[19] In our work, a 2 nm Cr layer was used and such an adhesion layer can be responsible for a spectral red-shift of about 30 nm. Other nanofabrication-related effects reported in a recent study can affect the spectral response of dipole plasmonic nanoantennas.[12]

Based on the analysis of the antennas SEM images, we found a close relation between the decreasing trend of the antenna's arm aspect ratio (AR) (length/width), with respect to the design values, and the decrease of the resonance peak position, as can be noticed in the inset of Fig. 5. The relation

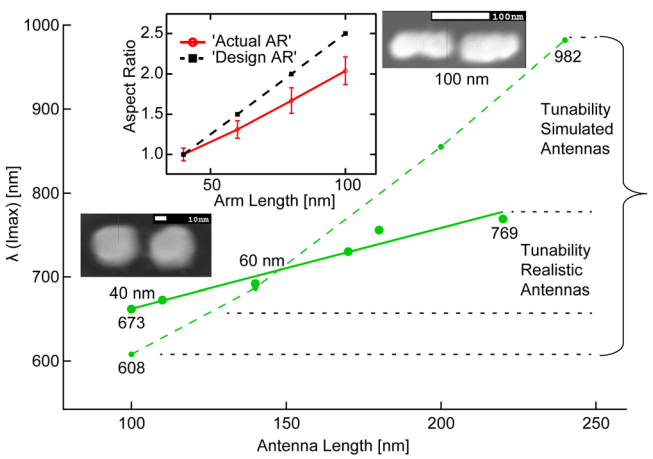

FIG. 5. Tunable range of realistic nanoantennas with 20 nm gap design. The hatched area on the bracket represents the effective tunable spectrum of antennas with length from 100 to 220 nm. SEM images illustrate the actual shapes for minimum and maximum arm lengths. The scale bars correspond to 10 nm for 40 nm and 100 nm for the largest antenna. The inset shows the intended and actual AR as a function of arm length.

between the aspect ratio and the plasmon resonance frequency (ω_{res}) of an elongated particle can be addressed through a simple mass-and-spring model.[20] Accordingly, $\omega_{res} = \omega_P/(2\sqrt{2}\ R)$, where ω_p represents the plasma frequency and R is the aspect ratio between length and width of the particle. Assuming the fact that the electric field of the charge distribution has a dipolar character,[20] the decrease of the aspect ratio leads to an increase of the restoring force acting on electron oscillations generated in the elongated NP. This result is in agreement with the blue-shift found for larger design patterns, as shown in the inset of Fig. 5.

Nevertheless, we believe that the main influence on the blue-shift comes from the shape effects due to the smoothness of the edges produced by the e-beam and the diffusion effects from Au deposition. Figure 6 shows the field intensity of nanoantennas with fixed length and gap of 60 and 20 nm, respectively, for different structural modifications. The results reveal the line-width and peak position dependence on the edge shape. More general observation of single silver NPs[21] has found that the effect largely depends on the original shape of the NPs. A single triangular NP was consecutively changed by heating to 200 °C, which caused to move the initial spectral peak centered at 625 nm to 585 nm after 30 min and, in a second cycle of 20 min, to 555 nm.[21]

We have approximated the shape modification observed in our nanoantennas by rounding the extremities of the arms of dipole nanoantennas. From the numerical calculations shown in Fig. 6, a blue-shift of about 40 nm of the resonance peak position with respect to the ideal cubic shape was confirmed when both the inner and outer faces of the arms were rounded. Slight changes are also observed when only one of the faces of the antennas is affected. The modeled shape modification resembles novel structures obtained by the combination of EB lithography and helium focused ion beam (He-FIB) milling.[22]

Therefore, we found that the spectral changes obtained for gold dipole nanoantennas due to these shape variations are in the order of those reported for single silver NPs.[21] The distribution of the electric field intensity at the corresponding resonance wavelength is shown in the right inset of Fig. 6.

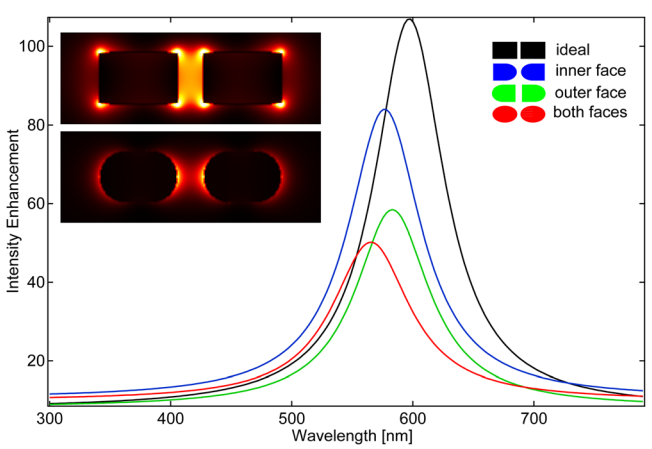

FIG. 6. Effect of the extremity shape on the spectral peak position. The black, green, blue, and red lines correspond to the ideal and rounded structures, as sketched in the inset. The left insets show the corresponding electric field intensity for an excitation along the main axis for the black and red structures.

A possible approach to address this phenomenon has been recently reported,[23] suggesting that the higher localization of the polarization charges at the center of the nanostructure surface is associated to a blue-shift of the spectrum. This may be originating from a reduction of the corners edge of the perfect cubic nanoantenna, leading to a decrease of the lightning-rod effects that causes the concentration of polarization charges at the corners of the nanostructure. Additionally, the presence of a neighboring nanostructure conforming the gap strongly attracts the opposite charges across the nanoscale gap and consequently increases the accumulation of polarization charges on the center of the nanostructure, thus reducing the resonance wavelength of the intra-particle oscillations.[24]

Studies, using gap structural modification, are recently reported for single NP spectroscopy, where variation of the coupling nature is achieved by controlling a residual gap width and height.[25] In other hands, the polarization conversion and coupling strength variation were demonstrated on L-shaped nanoantennas.[26]

In summary, we have investigated the variation in optical response of realistic nanoantennas respect to numerical simulations. The nanofabricated antennas were analyzed by SEM and have been found that the realistic nanoantennas have longer arms and smaller gaps compared to the nominal dimensions, which leads to a red-shift of the resonance peak. In addition and also due to fabrication limitations, realistic antennas have smoother edges than ideal structures and exhibit a decreasing aspect ratio for larger arm lengths, leading to a compensating blue-shift, as supported by calculations. All above hamper, the spectral tunability of the realistic nanoantennas compared to the ideal structures. These results are relevant to applications such as SERS, which require precise control of the spectral peak position for achieving high field enhancement.

The authors would like to thank Raziman Thottungal for his contribution with the SIE simulations. This work was supported by JSPS Core-to-Core Program, A. Advanced Research Networks.

[1]K. A. Willets and R. P. Van Duyne, Annu. Rev. Phys. Chem. **58**, 267 (2007).
[2]K. Kneipp, H. Kneipp, I. Itzkan, R. R. Dasari, and M. S. Feld, J. Phys.: Condens. Matter **14**(18), R597 (2002).
[3]A. Kinkhabwala, Z. Yu, S. Fan, Y. Avlasevich, K. Müllen, and W. E. Moerner, Nat. Photonics **3**, 654 (2009).
[4]A. L. Lereu, J. P. Hoogenboom, and N. F. van Hulst, Int. J. Opt. **2012**, 502930 (2012).
[5]T. R. Jensen, M. D. Malinsky, C. L. Haynes, and R. P. Van Duyne, J. Phys. Chem. B **104**, 10549 (2000).
[6]K. L. Kelly, E. Coronado, L. Zhao, and G. C. Schatz, J. Phys. Chem. B **107**, 668 (2003).
[7]E. Prodan, C. Radloff, N. J. Halas, and P. Nordlander, Science **302**, 419 (2003).
[8]P. Mühlschlegel, H.-J. Eisler, O. J. F. Martin, B. Hecht, and D. W. Pohl, Science **308**, 1607 (2005).
[9]H. Fischer and O. J. F. Martin, Opt. Express **16**, 9144 (2008).
[10]Y. Yao, M. Kats, R. Shankar, Y. Song, J. Kong, M. Loncar, and F. Capasso, Nano Lett. **14**, 214 (2014).
[11]Y. Alaverdyan, N. Vamivakas, J. Barnes, C. Lebouteiller, J. Hare, and M. Atatüre, Opt. Express **19**, 18175 (2011).
[12]C. Moosmann, G. Sigurdsson, M. Wissert, K. Dopf, U. Lemmer, and H. Eisler, Opt. Express **21**, 594 (2013).
[13]A. M. Kern and O. J. F. Martin, Nano Lett. **11**, 482 (2011).

[14]A. Horrer, C. Schäfer, K. Broch, D. Gollmer, J. Rogalski, J. Fulmes, and M. Fleischer, Small **9**, 3987 (2013).
[15]W. Zhang, H. Fischer, T. Schmid, R. Zenobi, and O. J. F. Martin, J. Phys. Chem. C **113**, 14672 (2009).
[16]A. Kern, A. Meixner, and O. J. F. Martin, ACS Nano **6**, 9828 (2012).
[17]P. B. Johnson and R. W. Christy, Phys. Rev B **6**, 4370 (1972).
[18]X. Jiao, J. Goeckeritz, S. Blair, and M. Oldham, Plasmonics **4**, 37 (2009).
[19]T. Siegfried, Y. Ekinci, O. J. F. Martin, and H. Sigg, ACS Nano **7**, 2751 (2013).
[20]P. Biagioni, J. S. Huang, and B. Hecht, Rep. Prog. Phys. **75**, 024402 (2012).
[21]J. J. Mock, M. Barbie, D. R. Smith, D. A. Schultz, and S. Schultz, J. Chem. Phys. **116**, 6755 (2002).
[22]O. Scholder, K. Jefimovs, I. Shorubalko, C. Hafner, U. Sennhauser, and G.-L. Bona, Nanotechnology **24**, 395301 (2013).
[23]T. V. Raziman and O. J. F. Martin, Opt. Express **21**, 21506 (2013).
[24]S. A. Maier, *Plasmonics: Fundamentals and Applications* (Springer, New York, 2007).
[25]Y. Wang, M. Abb, S. A. Boden, J. Aizpurua, C. H. de Groot, and O. L. Muskens, Nano Lett. **13**, 5647 (2013).
[26]L. J. Black, Y. Wang, C. H. Groot, A. Arbouet, and O. L. Muskens, ACS Nano **8**, 6390 (2014).